Electronic Supplementary Information

Metal-Polydopamine Frameworks and their Transformation to Hollow Metal/N-doped Carbon Particles

*Yan Liang, Jing Wei, Yaoxin Hu, Xiaofang Chen, Jin Zhang, Xinyi Zhang, San Ping Jiang, Shanwen Tao and Huanting Wang**

EXPERIMENTAL

Chemical reagents

Cobalt nitrate hexahydrate, Zinc nitrate hexahydrate, 2-methylimidazole (2-mim), Dopamine hydrochloride are purchased from Sigma-Aldrich without further purification. Ethanol 99.7%, Methanol GR and tris(hydroxymethyl)aminomethane are from Merck. Reverse Osimosis water was used for all solution preparations. Oxygen (Airgas, 99.999%) and Argon (Airgas, 99.999%) were used for carbonization and electrochemical test.

Synthesis of ZIF-67 and ZIF-8

1.455 g of $Co(NO_3)_2{\cdot}6H_2O$ and 1.65 g of 2-mim was dissolved in 20 ml of methanol, respectively. Then $Co(NO)_3$ and 2-mim methanol solution was poured into 60 ml of methanol, stirring for 3 h at room temperature. The result ZIF-67 powder was collected by centrifugal washing 3 times with methanol and drying in vacuum at 60 °C overnight.

0.915 g of $Zn(NO_3)_2$ $6H_2O$ dissolved in 30 ml of methanol mixed with 50 ml of methanol dissolved 2.025 g of 2-mim, stirring for 3 h at room temperature. The result ZIF-8 powder was collected by centrifugal washing 3 times with methanol and drying in vacuum at 60 °C overnight.

Preparation of Hollow Metal-Dopamine Nanoparticles (Z67D)

10 mg of ZIF-67 (size around 500 nm) was dispersed in a mixed solution of ethanol (20 mL) and water (15 mL) under ultrasonication. Dopamine (4 mg) was then added into above mixture solution with magnetic stirring. After stirring for 5 min, 10 mL of aqueous solution of Tris(hydroxymethyl)aminomethane (25 mM) was added. The reaction proceeded under magnetic stirring for 48 h at room temperature. The sample was washed by centrifugation with deionized water and ethanol three times and finally dried in vacuum at 60 °C overnight. The obtained product was denoted as Z67D.

Preparation of Hollow Metal-Dopamine Nanoparticles (Z8D)

10 mg of ZIF-8 (size around 60 nm) was dispersed in a mixed solution of ethanol (20 mL) and water (15 mL) under ultrasonication. Dopamine (40 mg) was then added into above mixture solution with magnetic stirring. After stirring for 5 min, 10 mL of aqueous solution of Tris(hydroxymethyl)aminomethane (25 mM) was added. The reaction proceeded under magnetic stirring for 24 h at room temperature. The sample was washed by centrifugation with deionized water and ethanol three times and finally dried in vacuum at 60 °C overnight. The obtained product was denoted as Z8D.

Preparation of hollow carbon structures

The resulting Z67D powder was heated to 600 °C, 700 °C and 800°C at a rate of 5 °C/min and maintained at these temperatures for 3 h. After cooling down to room temperature, the resulting powder was mixed with HCl (2 M) at room temperature under stirring for 12 h to remove the unconjugated cobalt. After centrifugation and washing with water for several times, Co/CoN$_x$ hollow carbon structures were obtained after dried at 60 °C overnight.

The resulting Z8D powder was heated to 900 °C at a rate of 5 °C/min and maintained at these temperatures for 3 h. The N doped hollow carbon structures were obtained after powder cooling down to room temperature.

Characterization

Scanning electron microscopy (SEM) images were carried out on a FEI Magellan 400 field emission scanning electron microscope operating at 5 kV. The transmission electron microscopy (TEM) images were taken by FEI Tecnai G2 T20 and the elements mapping is acquired by Scanning Transmission electron microscopy (STEM) on FEI Tecnai G2 F20 FEGTEM operated at an accelerating voltage of 200 kV. Nitrogen sorption isotherms were measured at 77 K with a Micromeritic Tri Flex surface characterization analyzer. Before measurements, the samples were degassed in vacuum at 180 °C for at least 8 h. Powder X-ray diffraction (XRD) patterns were carried out on a Miniflex 600 diffractometer (Rigaku, Japan) in transmission geometry equipped with Cu Kαradiation (15 mA and 40 kV) at a scan rate of 2° min^{-1} and a step size of 0.02°. Samples were ground with KBr and pelletized for analysing by Fourier transform infrared spectra (FTIR) spectrophotometer (PerkinElmer Spectrum 100, USA). X-ray photoelectron spectroscopy (XPS) experiments were carried out on a Kratos AXIS Ultra DLD system with Al Kα radiation as an X-ray source for radiation. The total surface area and pore volume were calculated by using Brunauer-Emmett-Teller (BET) method and Density functional theory (DFT) method, respectively.

Electrochemical method

All electrochemical measurements including cyclic voltammetry (CV) and linear scan voltammogram (LSV) were carried out by using a μAutolab electrochemical analyzer in a conventional three-electrode electrochemical cell at room temperature. A Pt wire and a saturated Ag/AgCl (saturated with 3 M KCl) were used as counter electrode and reference electrode, respectively. All potentials refer to the reversible hydrogen electrode (RHE). Rotating disk glassy carbon electrode (5 mm diameter, 0.196 cm^2) served as the substrate for working electrode to evaluate the ORR activity.

The catalyst ink was prepared by dispersing 10 mg nanocatalyst materials (or commercial Pt/C (20 wt.%) from Sigma-Aldrich) in 0.9 ml ethanol and 100 μL Nafion solution (0.5 wt.%) under ultrasonication. Then a certain volume of catalyst ink was pipetted on the surface of the pre-cleaned rotating disk electrode to result in a desirable catalyst loading and dried at room temperature. CV tests measured in Ar-saturated and O_2-saturated 0.1 M KOH solution with a sweep rate of 50 mV/s, respectively. While the rotating disk electrode (RDE) tests were all measured in O_2-saturated 0.1 M KOH solution with a sweep rate of 10 mV/s. A flow of O_2 was maintained over the electrolyte during the CV and LSV test to ensure O_2 saturation.

For the ORR, the electron transfer numbers (n) can be calculated by Koutecky-Levich equation, at various electrode potentials:

$$\frac{1}{J}=\frac{1}{J_L}+\frac{1}{J_K}=\frac{1}{B\omega^{0.5}}+\frac{1}{J_K}$$

$$B=0.62nFC_0D_0^{2/3}v^{-1/6}$$

where J is the measured current density; J_K and J_L are the kinetic and diffusion-limiting current densities, respectively, ω is the angular velocity of the disk, n is transferred electron number, F is the Faraday constant (96485 C mol^{-1}), C_0 is the bulk concentration of O_2 (1.2×10^{-6} mol cm^{-3}), D_0 is the diffusion coefficient of O_2 in 0.1 M KOH (1.9×10^{-5} cm^2 s^{-1}), and ν is the kinematic viscosity of the electrolyte (0.01 cm^2 s^{-1}).

Figures S1-22

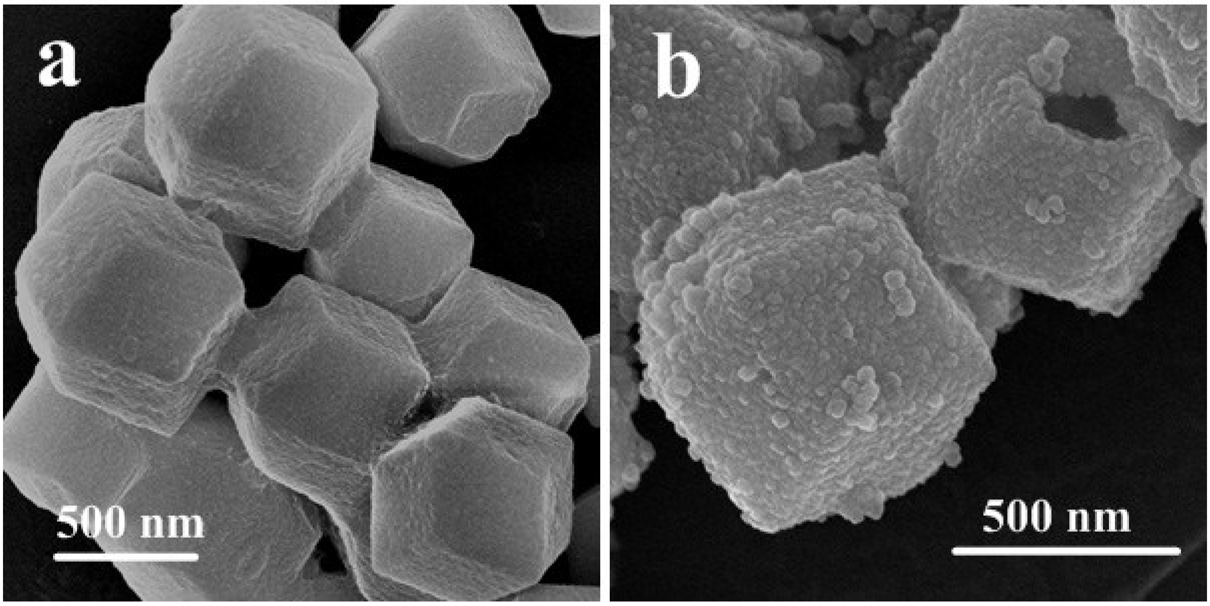

Figure S1. SEM images of ZIF-67 and Z67D.

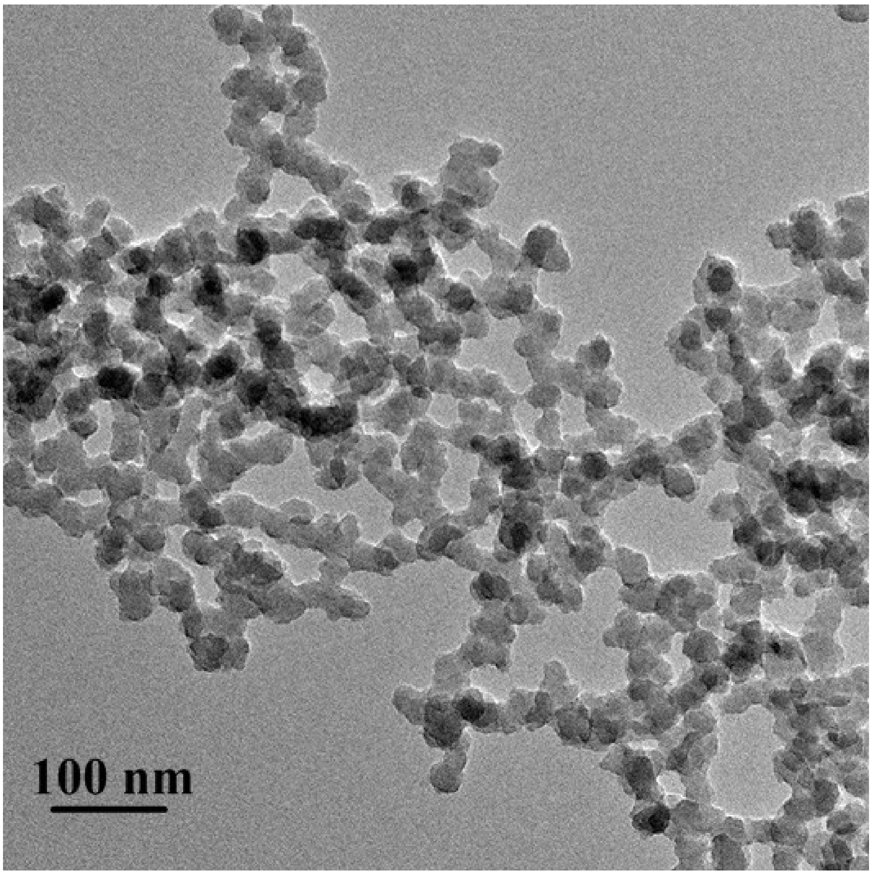

Figure S2. TEM image of $Co(NO_3)_2 \cdot 6H_2O$ mixed with dopamine in water and ethanol solution for 24 h.

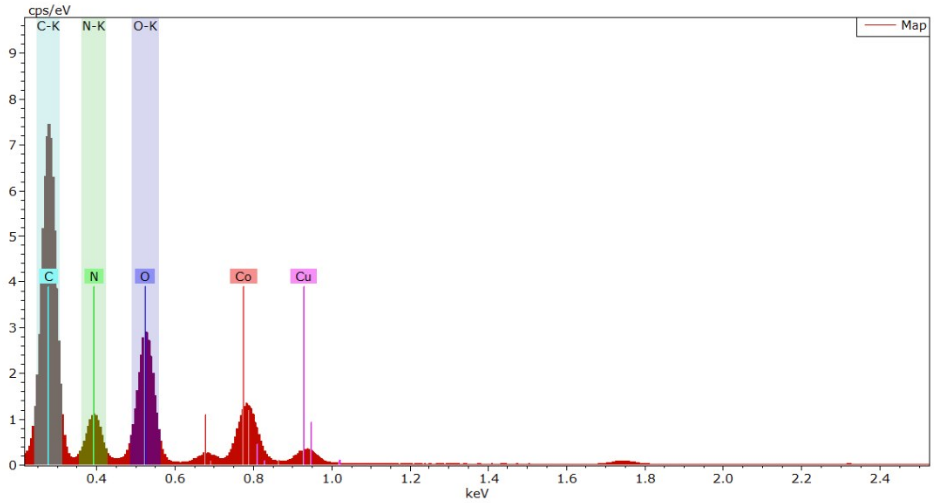

Figure S3. EDS spectrum of Z67D.

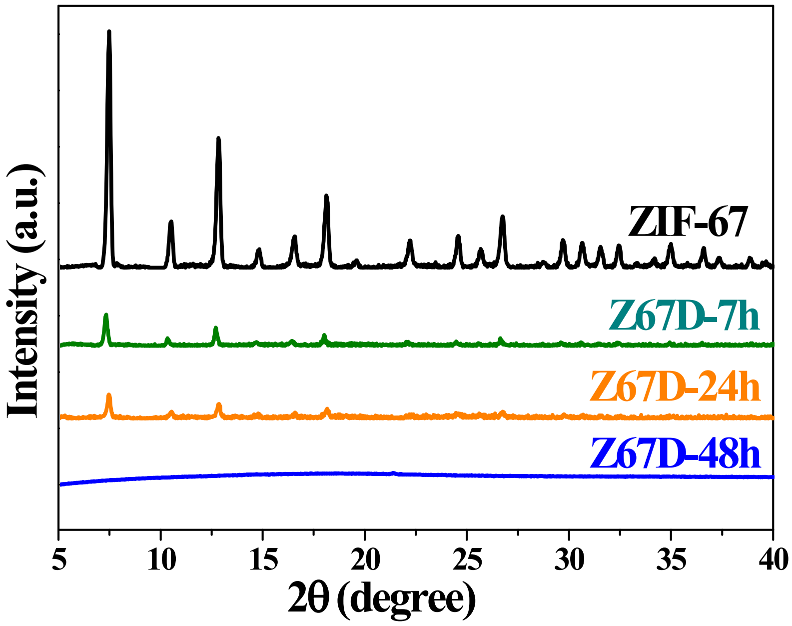

Figure S4. XRD patterns of ZIF-67 and hollow Z67D structure formed at different time.

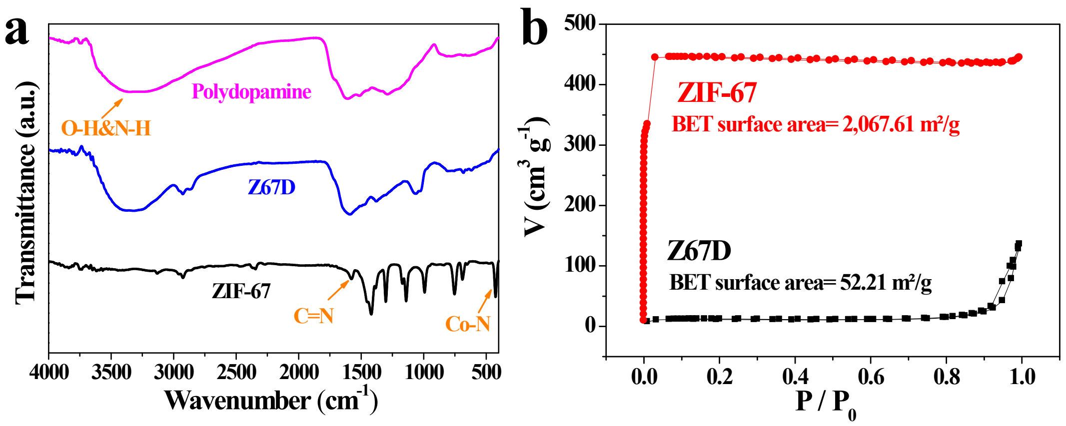

Figure S5. (a) FTIR spectrums of PDA, Z67D, and ZIF-67. (b) N_2 sorption isotherms and BET surface area of ZIF-67 and Z67D.

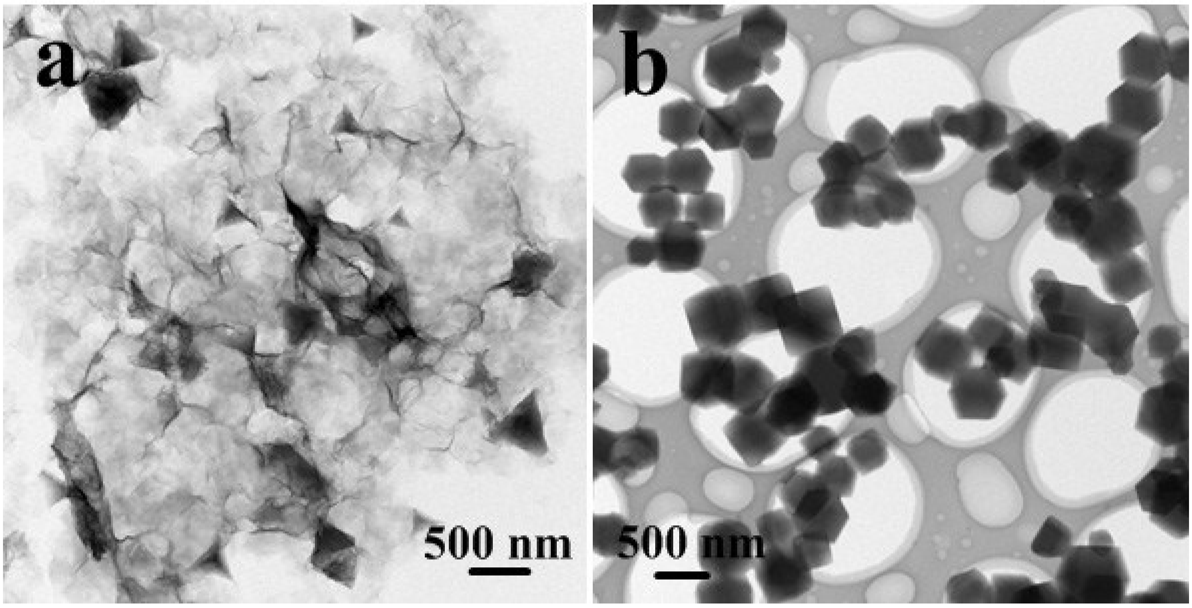

Figure S6. TEM images of ZIF-67 nanoparticles stirred in solution of water and ethanol (a) and in ethanol (b) for 24 h.

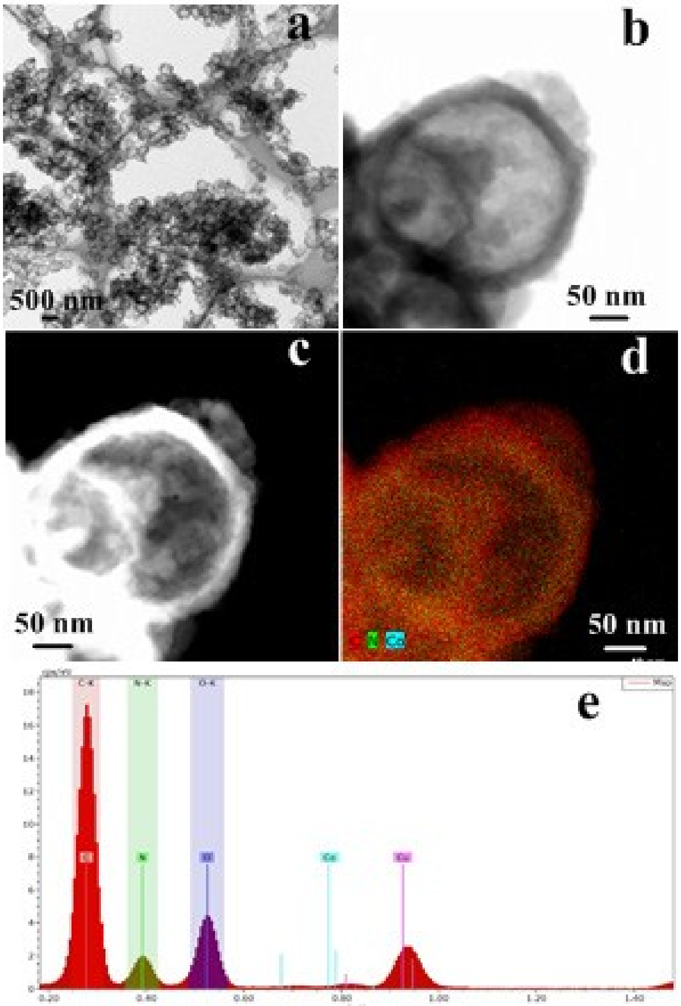

Figure S7. (a) TEM image of Z67D after mixing with 6 M HCl for 24 h. (b-e) STEM, EDS mapping images and spectrum of Z67D after being washed by acid.

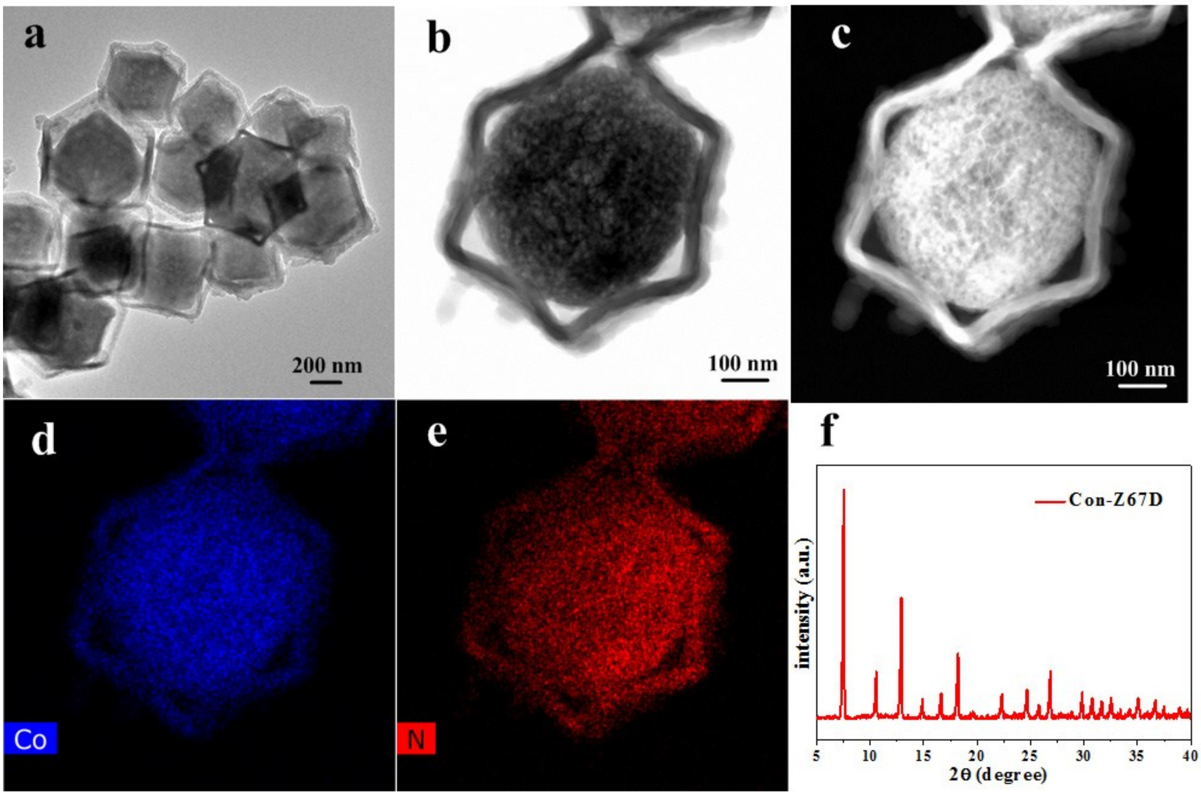

Figure S8. (a) TEM image of Z67D synthesized under concentrated solution of water and ethanol (Con-Z67D). (b-c) STEM, (d-e) elements mapping images and (f) XRD pattern of Con-Z67D.

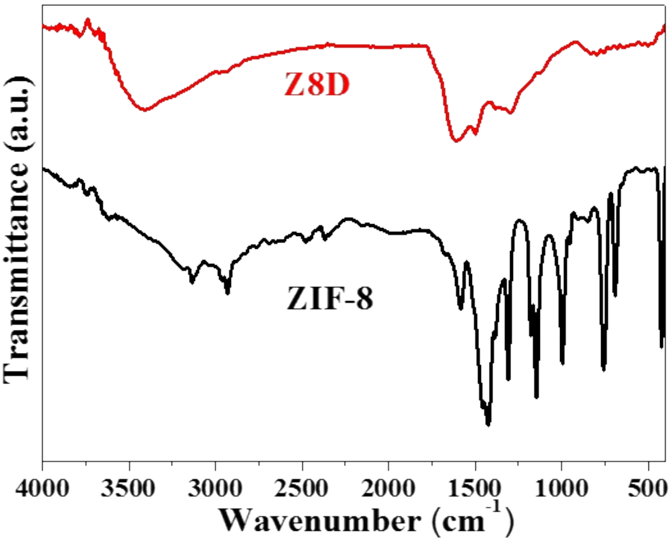

Figure S9. FTIR spectrums of ZIF-8 and Z8D.

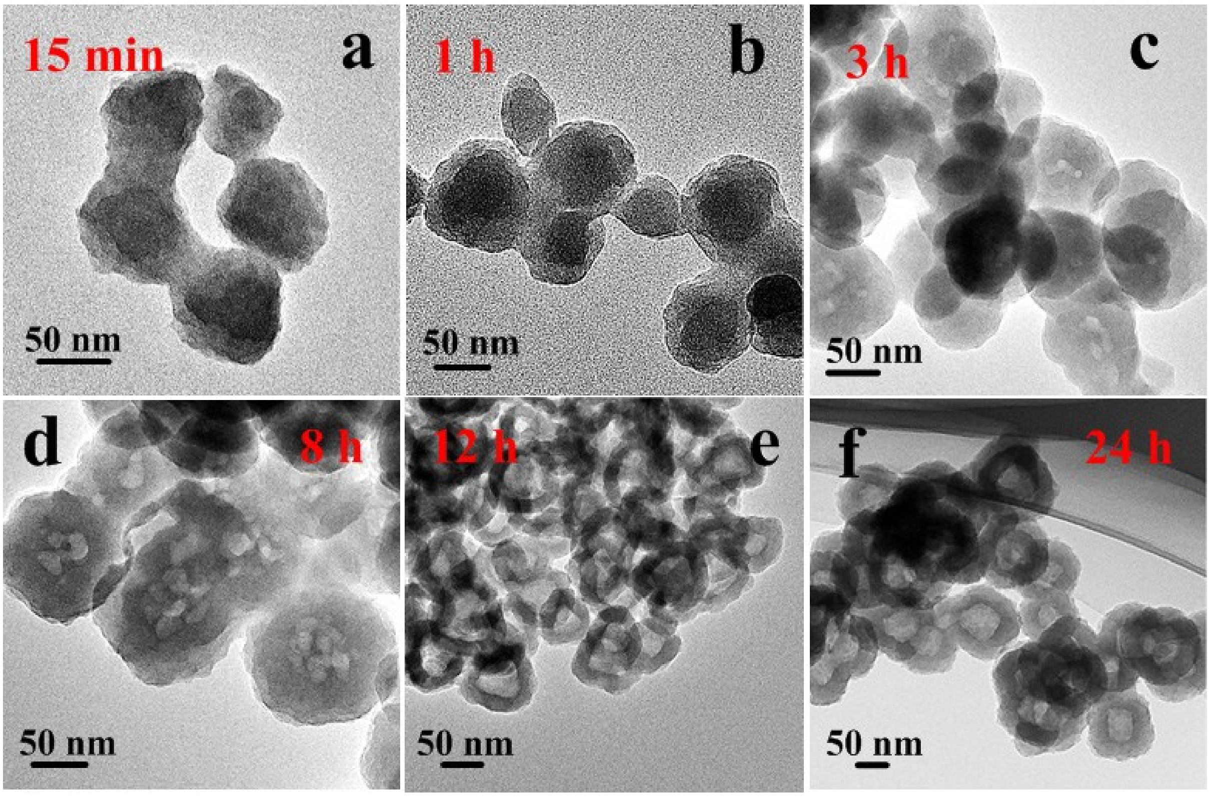

Figure S10. TEM images at each stage of hollow Z8D structures formation process.

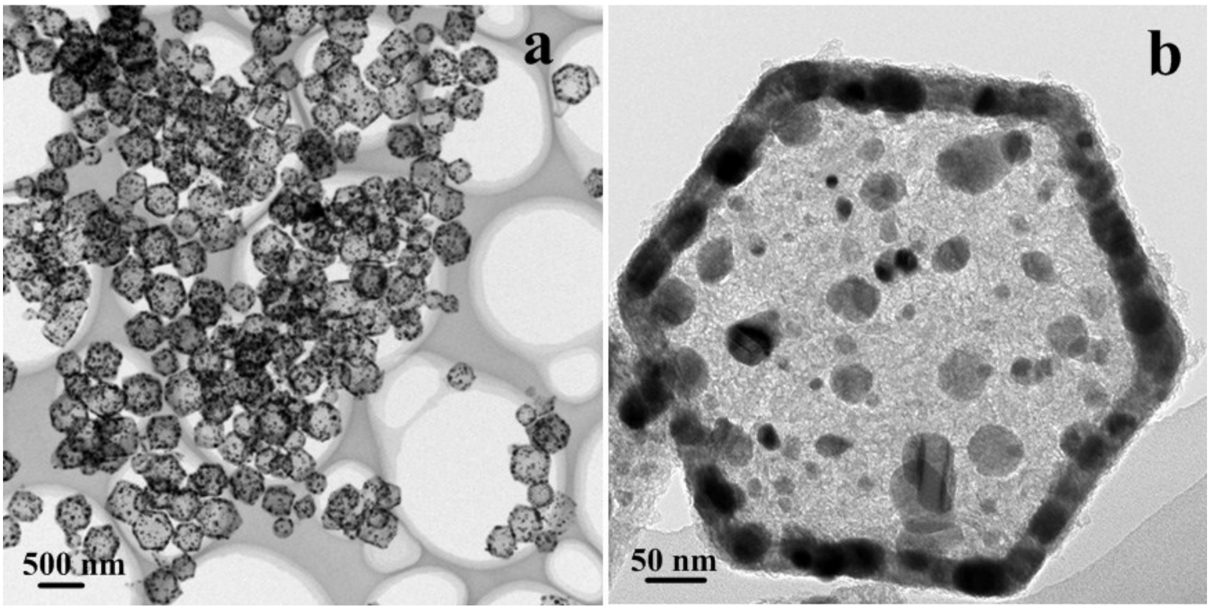

Figure S11.TEM images of Z67D after carbonization at 700 °C in Ar atmosphere.

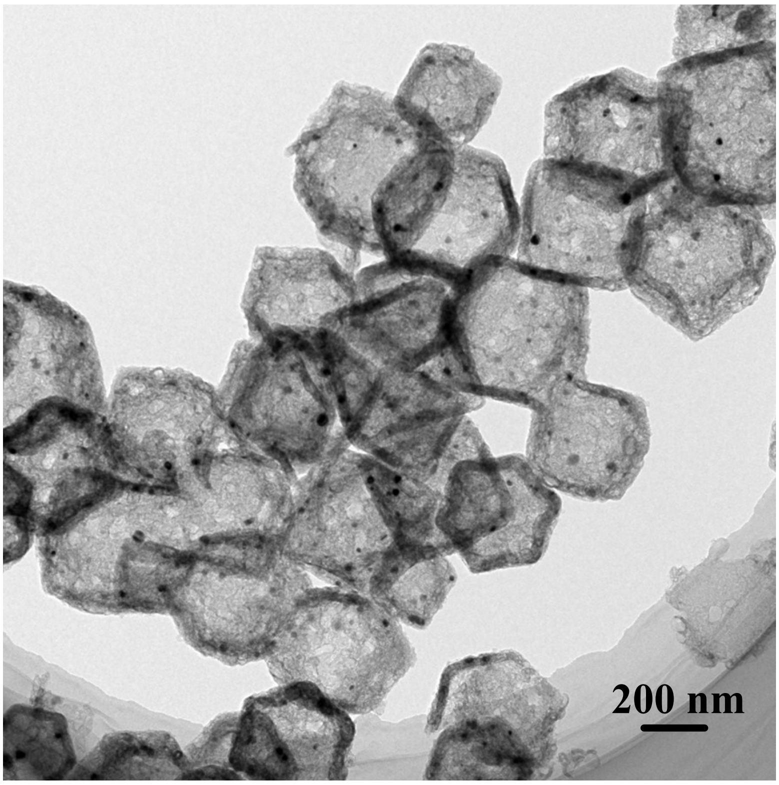

Figure S12.TEM images of Z67D-700 after acid leaching.

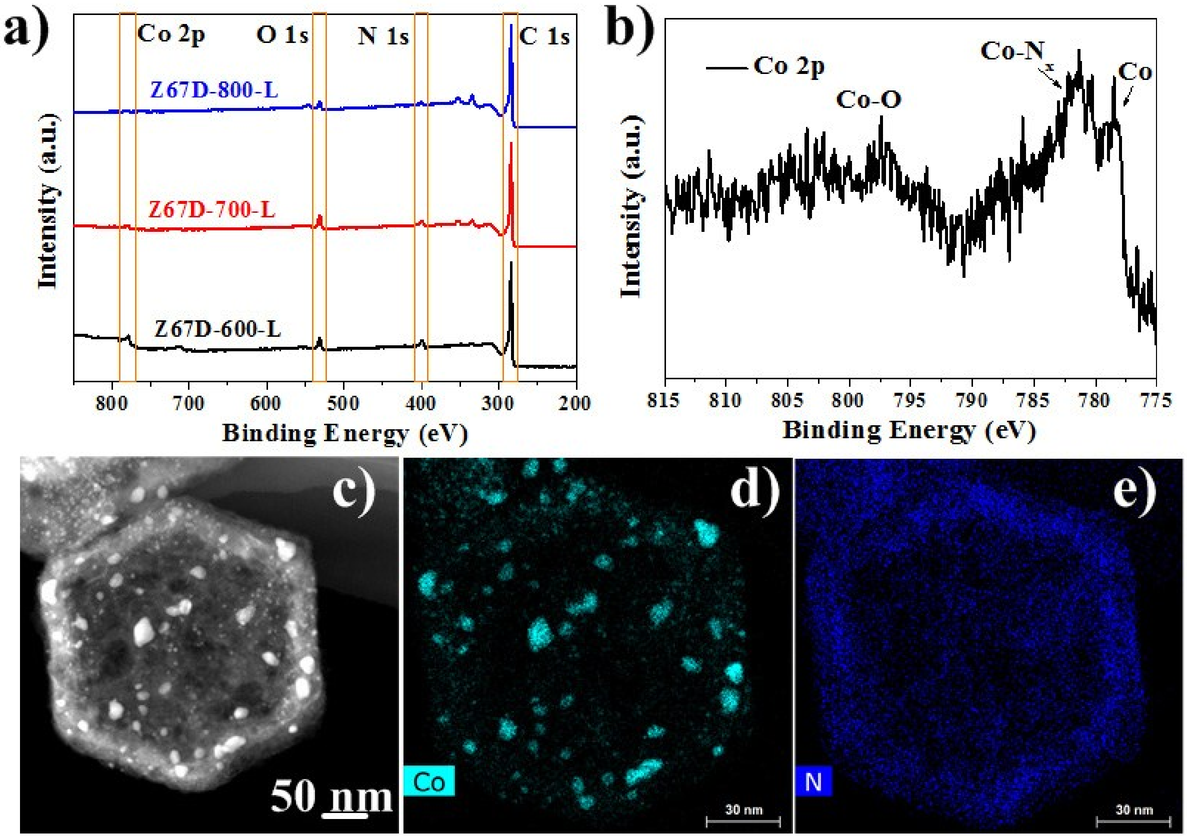

Figure S13. (a) XPS spectrum of Z67D-600-L, Z67D-700-L and Z67D-800-L; (b) High resolution XPS spectrum of Co 2p of Z67D-700-L; (c) STEM and element mapping images (d, e) of Z67D-700-L.

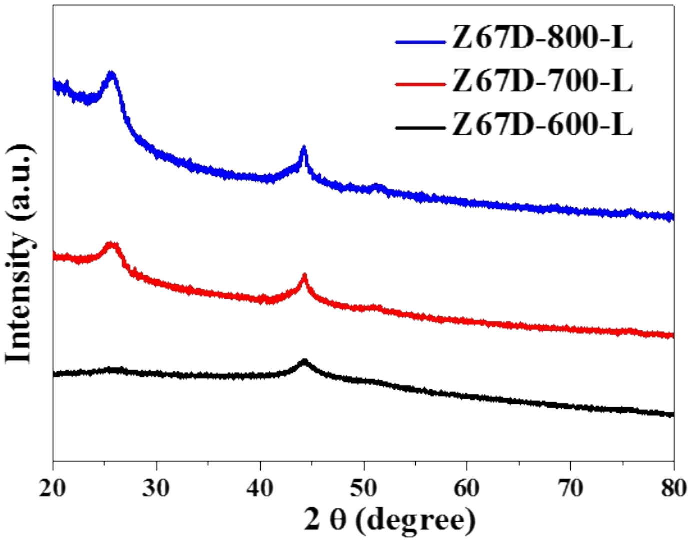

Figure S14. XRD patterns of Z67D-600-L, Z67D-700-L and Z67D-800-L.

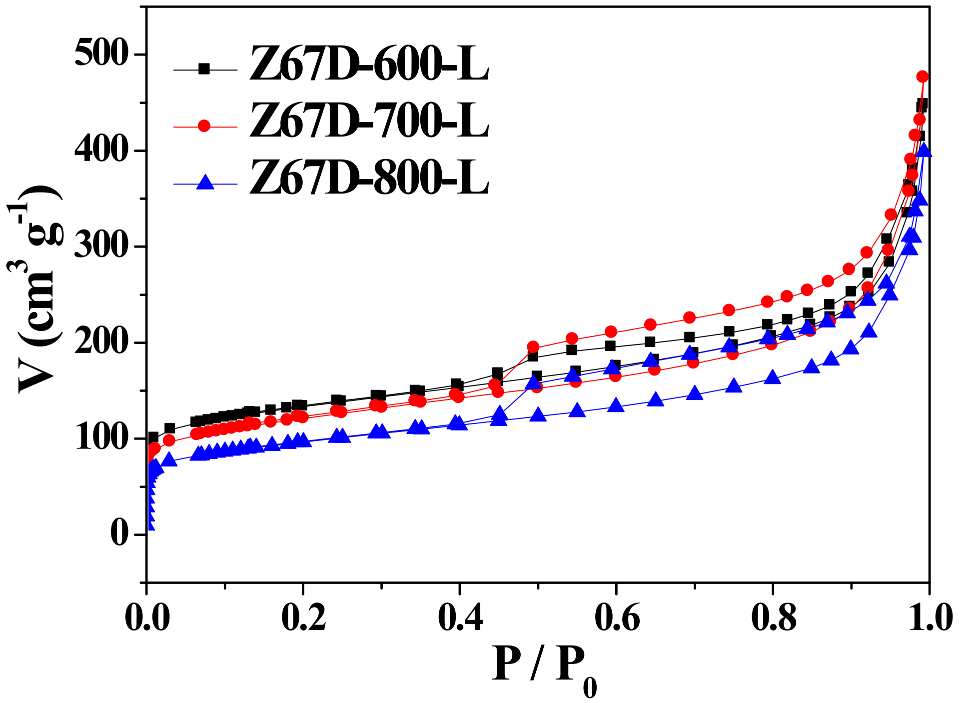

Figure S15. N_2 sorption isotherms of Z67D-600-L, Z67D-700-L and Z67D-800-L.

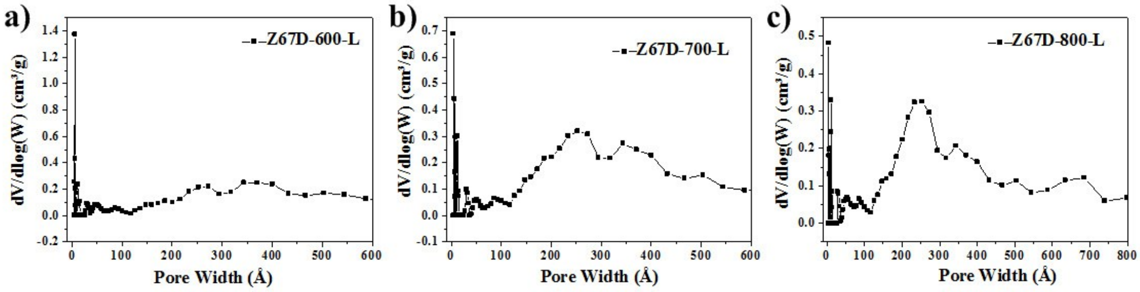

Figure S16. Pore size distribution for Z67D-600-L (a), Z67D-700-L (b) and Z67D-800-L (c) based on the density functional DFT method.

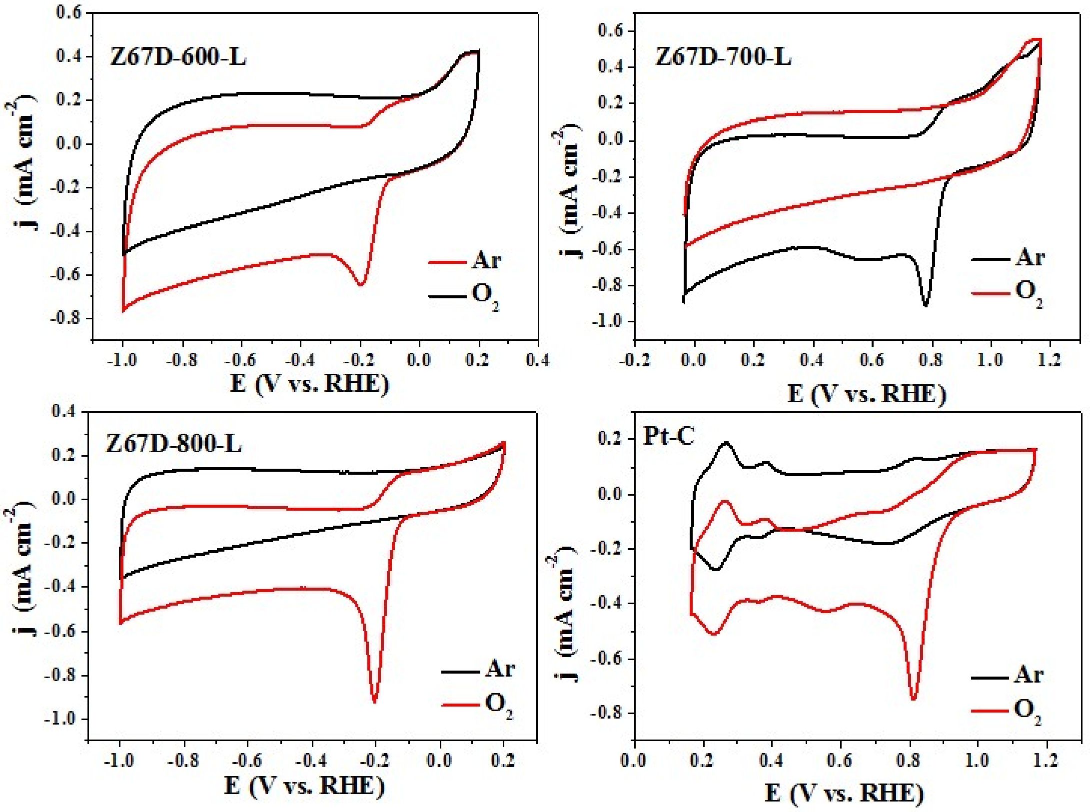

Figure S17. CV curves of Z67D-600-L, Z67D-700-L, Z67D-800-L and Pt/C in Argon-saturated and Oxygen-saturated 0.1 KOH solution.

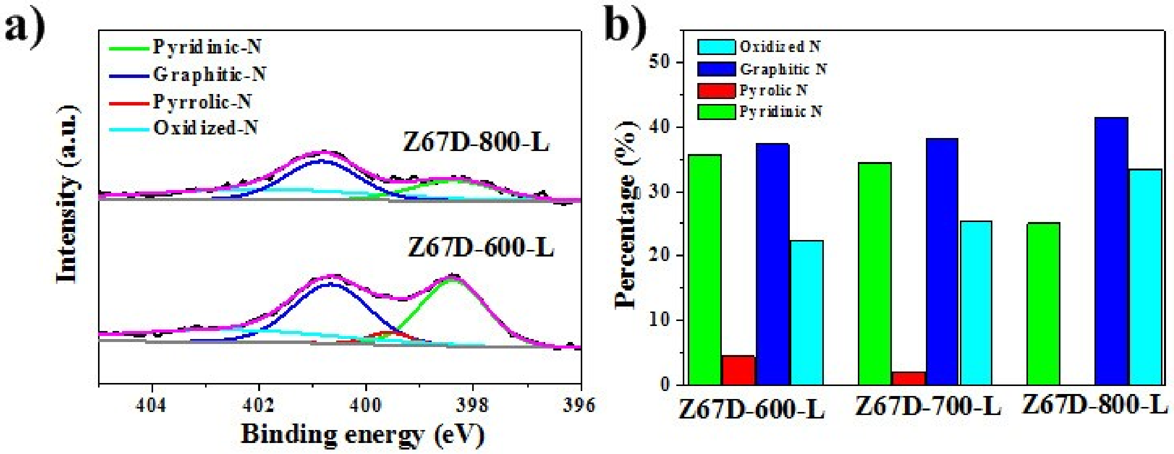

Figure S18. (a) High-resolution XPS spectra of N 1s for Z67D-600-L and Z67D-800-L. (b) Normalized ratios of pyridinic N, pyrrolic N, graphitic N, and oxidized pyridinic nitrogen, in Z67D-600-L, Z67D-700-L and Z67D-800-L from the XPS results in Figure 5b and Figure S18a.

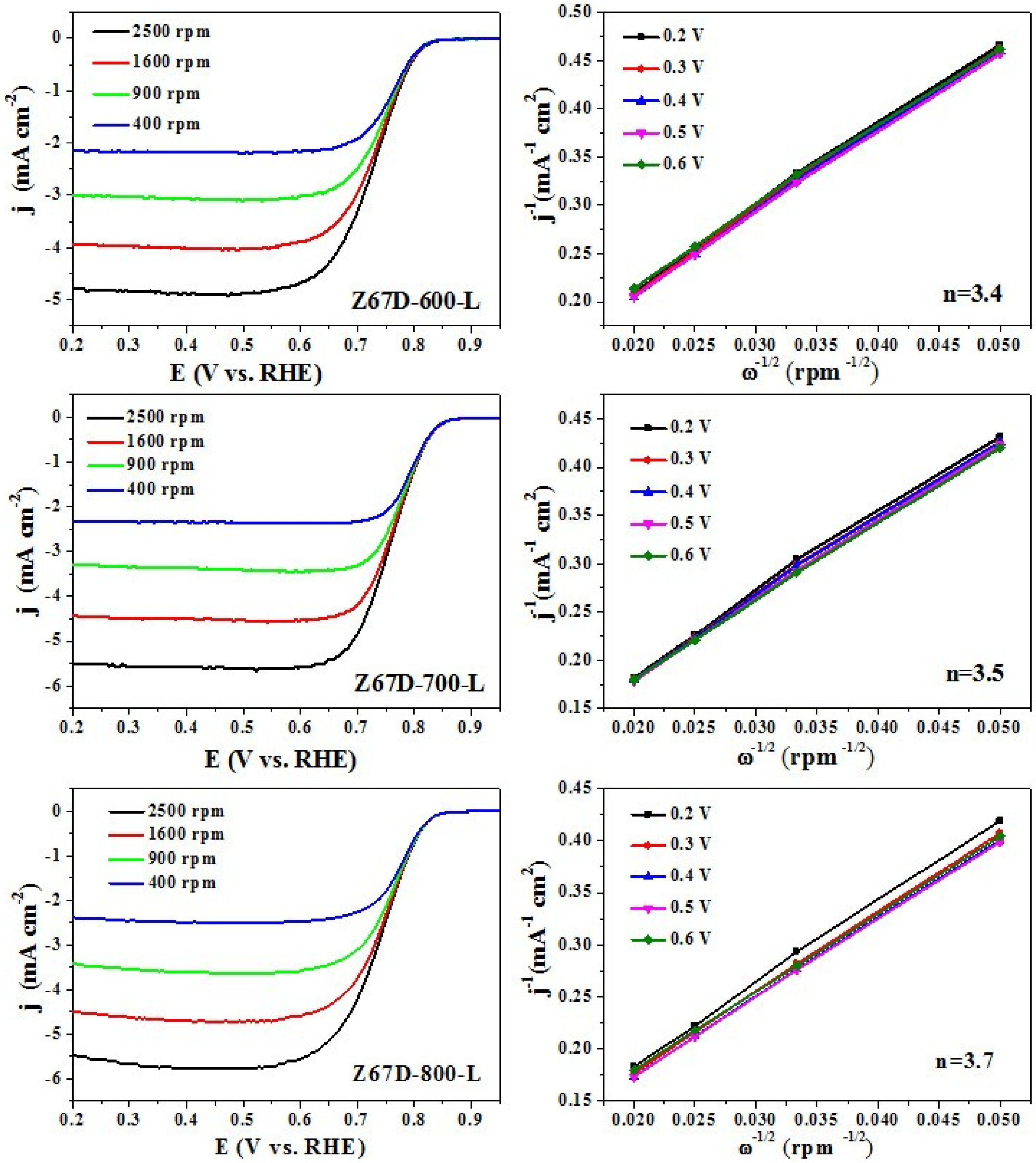

Figure S19. LSV curves and corresponding K-L plots and electron transfer numbers of (a, b) Z67D-600-L, (c, d) Z67D-700-L and (e, f) Z67D-800-L.

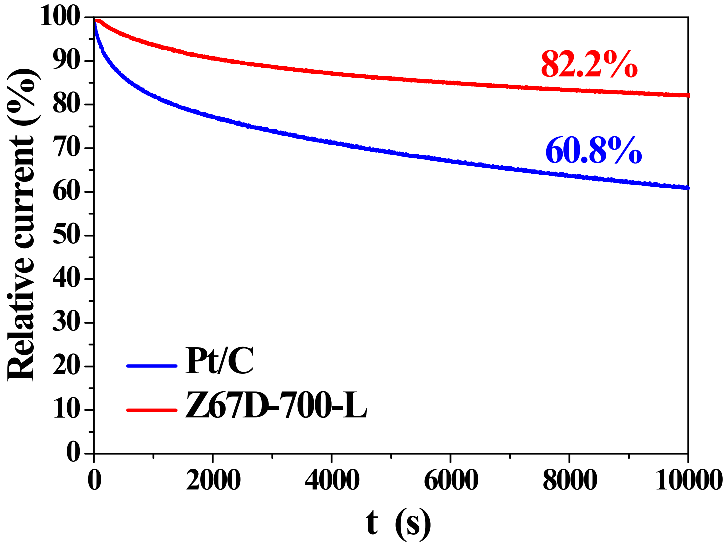

Figure S20. Current-time chronoamperometric response of Z67D-700-L and Pt/C under 1600 rpm in O_2-saturated 0.1 M KOH at 0.77 V.

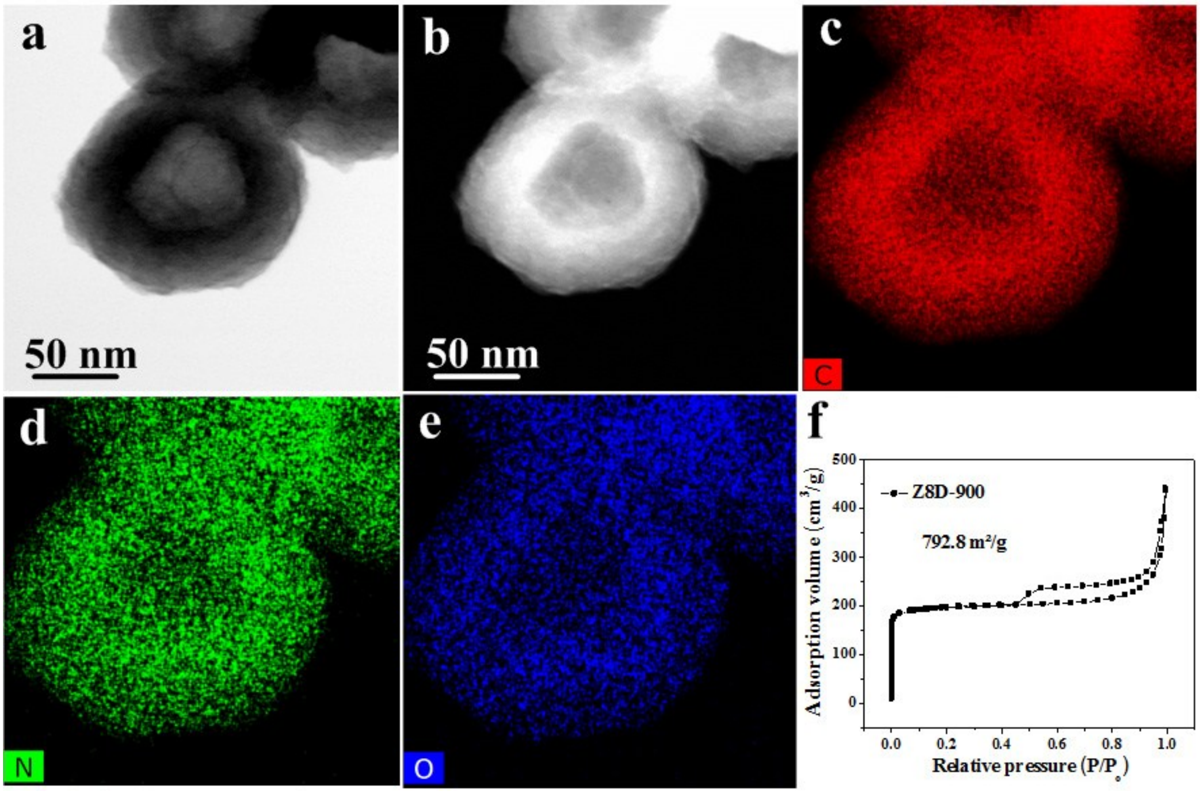

Figure S21. (a-e) STEM image and EDS mapping of Z8D-900. (f) Nitrogen sorption isotherms and BET surface area of Z8D-900.

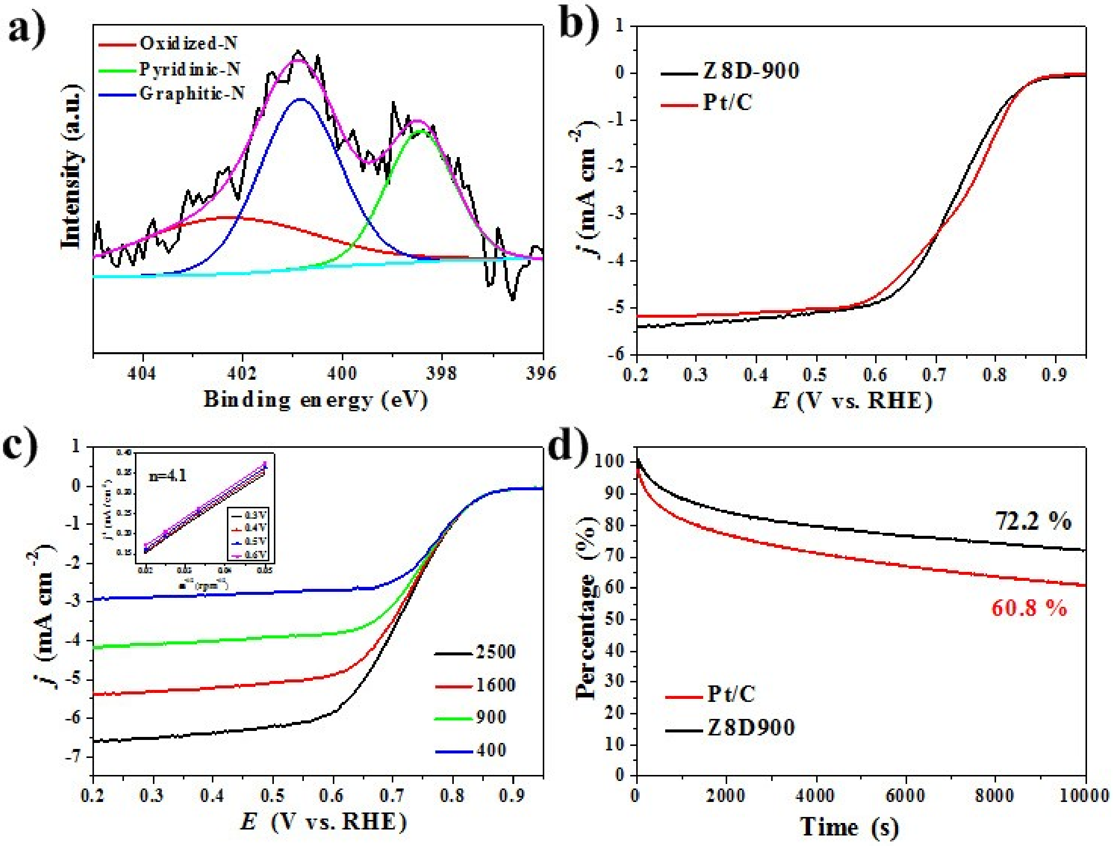

Figure S22. (a) High resolution of N 1s spectra of Z8D-900, (b) LSV curves of Z8D-900 with 0.2 mg cm^{-2} loading, (c) K-L plots and electron transfer numbers of Z8D-900, (d) Current-time chronoamperometric response of Z8D-900 and Pt/C under 1600 rpm in O_2-satureated 0.1M KOH at 0.77 V.

Figure S22a shows the three types of nitrogen of N1s in Z8D-900. Nitrogen doping and its high surface area gives Z8D-900 more active sites and rapid transportation of ORR-relevant species, which means high ORR electrocatalytic activity. As show in Figure S22b, its onset potential is around 0.86 V, which is almost as good as Pt/C, even without metal doping. The electron transfer number, calculated from the LSV curves by using K-L equation in Figure S22c, is around 4. This value indicates ideal four-electron reaction pathways for the direct reduction of O_2 to OH^- instead of HO_2^- on the electrode. The stability of Z8D-900 was also assessed in Figure S22d.